Conformational dynamics of a metallomesogen studied by ^{2}H-NMR spectroscopy

Ronald Y. Dong and C. R. Morcombe
Department of Physics and Astronomy, Brandon University, Brandon, Manitoba, Canada R7A 6A9

L. Calucci, M. Geppi, and C. A. Veracini
Dipartimento di Chimica e Chimica Industriale, Università degli Studi di Pisa, Via Risorgimento 35, 56126 Pisa, Italy

(Received 1 September 1999)

In this work we present a quantitative analysis of both quadrupolar splittings and deuterium Zeeman and quadrupolar spin-lattice relaxation times reported in the literature for two isotopomers of Azpac, an acetylacetonate derivative of the cyclopalladated 4,4'-bis(hexyloxy) azoxybenzene. Azpac-d_4 is deuterated at the aromatic rings and Azpac-d_{26} is deuterated on the alkoxy chains. The additive potential method is used to model the splittings, while the derived spectral densities are interpreted using the decoupled model in conjunction with the Nordio model. The two side chains are assumed to be noninteracting and identical in their conformations in order to limit the size of the transition rate matrix needed to describe correlated internal bond rotations in the chains. Rotational diffusion constants and internal jump rate constants are derived for this metallomesogen.

PACS number(s): 61.30.Cz, 61.30.Eb, 64.70.Md, 76.60.−k

I. INTRODUCTION

Metal containing liquid crystals, known as metallomesogens [1], are of interest because of their potential technical applications. Peculiar characteristics of metallomesogens are their high transition temperatures, poor thermal stability, and high viscosity. Hence, data concerning their physical properties are scarce in the literature. Among metallomesogens, the acetylacetonate derivative of the cyclopalladated 4,4'-bis(hexyloxy) azoxybenzene (Azpac) is an exception, showing a nematic phase below 100 °C. Thus Azpac has been extensively investigated to determine some physical properties such as refractive indices [2], elastic and viscosity constants [3], dielectric permitivities [4], and flexoelectric coefficients [5]. Recently, deuterium NMR spectra were recorded [6,7] in the nematic phase of two isotopomers of Azpac: one deuterated in the positions 3 and 5 of both rings (Azpac-d_4) and the other deuterated in the hexyloxy chains (Azpac-d_{26}) and their interpretations were given. In addition, deuteron Zeeman (T_{1Z}) and quadrupolar (T_{1Q}) spin-lattice relaxation times were reported by us [7] for these isotopomers. The derived spectral densities $J_1(\omega_o)$ and $J_2(2\omega_o)$ at $\omega_o/2\pi = 46$ MHz for Azpac-d_4 were explained by the small step rotational diffusion model of Nordio *et al.* [8], while those measured in Azpac-d_{26} remained to be analyzed. It was noted that the quadrupolar splittings and relaxation behavior of the two alkoxy chains show distinguishable features despite overlaps of some spectral lines in the ^{2}H-NMR spectrum. Although many studies of liquid crystal molecules in mesophases have been performed [9] using ^{2}H-NMR spectroscopy, the molecules studied to unravel both the order and relaxation behaviors have a ''single'' side chain [10–14] or several identical side chains [15]. Hence, Azpac presents an interesting and challenging task for the decoupled model [16,17] to unravel the conformational dynamics. Indeed when both hexyloxy chains are considered simultaneously, the number of configurations available to Azpac is incredibly huge ($>59\,000$) and simplifying assumptions must be made in fitting the quadrupolar splittings using the additive potential (AP) method [18] and the spectral density data in particular. This work represents our effort to quantitatively analyze all the NMR observables in Azpac-d_4 and Azpac-d_{26}. The major assumption to limit the number of configurations to 243 [10,14,15] is to make both chains (A and B) identical and noninteracting for modeling the intermolecular potential of mean torque, while transitions among different configurations can be described using one chain (chain A or B) only. This makes the Azpac problem tractable and the results are presented in this paper.

The reorientation of molecules in liquid crystals can be described by the rotational diffusion model [8,19]. The model assumes a stochastic Markov process for reorientation in which each molecule moves in time as a sequence of small angular steps caused by collisions with its surrounding molecules and under the potential of mean torque set up by them. Nordio *et al.* [8] considered reorientation of cylindrical, rigid molecules in uniaxial phases. Each molecule is characterized by a rotational diffusion tensor, normally defined in a frame fixed on the molecule. A number of models of increasing complexity has been proposed [20–24]. For biaxial molecules like Azpac reorienting in uniaxial phases, the Tarroni-Zannoni model [22] seems in principle more appropriate. However, the tumbling motion of Azpac [7] was estimated to be very slow (10^3 s^{-1}) and it is doubtful whether the relaxation data can detect a nonaxial rotational diffusion motion in this case. Furthermore, the molecular biaxiality of Azpac is found (see below) to be very small. Hence, the Nordio model is used as before [7]. Internal ring rotations of ring B about its para axis (see Fig. 1) can be superimposed onto the reorientation of the molecule in the small step diffusion limit [25] or in the strong collision limit [26]. As before [7], the small step diffusion limit for free ring rotations is used for ring B of Azpac.

Correlated internal rotations in flexible chains of several liquid crystals have been studied by measurements of ^{2}H-NMR relaxation times and successfully modeled [9–15]

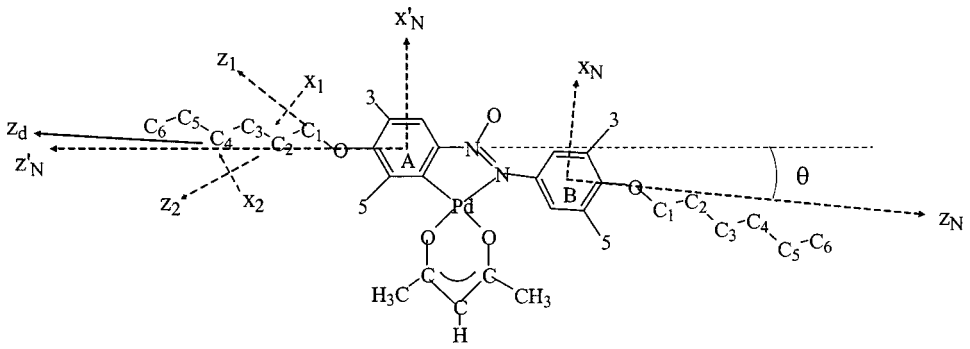

FIG. 1. Molecular structure of Azpac showing various coordinate systems used in the text. Sites 3 and 5 on rings *A* and *B* are deuterated in Azpac-d_4. The long molecular z_d axis makes a 1° angle with the z'_N axis.

using the decoupled model [16] in which conformational dynamics in the side chain is assumed to be independent of the orientation of the molecule. All possible configurations in a flexible chain are generated by the rotational isomeric state (RIS) model of Flory [27]. In the time domain, a master equation is constructed to describe transitions among all configurations available to the molecule. The master rate equation is solved as an eigenvalue problem by diagonalizing a rate matrix which contains jump rate constants for one- (k_1), two- (k_2), and three-bond (k_3) motions. A one-bond motion involves rotation of the last carbon-carbon (C–C) bond in the chain, while a two-bond rotation is defined as the rotation of the penultimate bond (C_4-C_5 in a hexyloxy chain) with all the other C–C bonds in the chain remaining the same except the last one, which may or may not rotate. A three-bond rotation is the interchanging of two alternate (i.e., next-nearest-neighbor) bonds, which is the well known crankshaft motion in the chain. These elementary jump constants are phenomenological model parameters used to mimic internal chain dynamics. It is noted that in our decoupled model, a single ''average'' rotational diffusion tensor is assumed. In other words, rotational diffusion tensors for different conformers do not deviate substantially from each other. This is a consequence of a massive aromatic core in comparison with its side chain(s). Order director fluctuations [9] are another possible relaxation mechanism in liquid crystals, but their contributions are often negligible in the MHz region. Our data were collected at 46 MHz, thereby making order director fluctuations unnecessary in the present study.

The paper is organized as follows. Section II outlines an extension of the basic theory appropriate for analyzing both the quadrupolar splittings and spectral density data in the nematic phase of Azpac. Section III describes results and discussion, while Sec. IV gives a brief summary.

II. BASIC THEORY

In this section we outline the necessary procedures and formulas for discussing the measured quadrupolar splittings and spectral densities of motion. The molecular mean field theory based on the AP method has been well documented [9,18] in the literature, while the decoupled model [9,11,16] has been recently proposed. The geometry used to describe the C–C backbone of the alkoxy chains is identical to those used before [28], i.e., $\angle$ CCH=107.5°, $\angle$OCC=$\angle$CCC =113.5°, $\angle$HCH=113.6°. The dihedral angles for rotation of a C–C bond in the chain are $\phi=0,\pm 112°$ for the three RISs. These correspond to the *trans* (t), and two symmetric *gauche* ($g\pm$) states. The *gauche* states have higher internal energy E_{tg}(CCC) in comparison to that of the *trans* state. When the chain contains a g^+g^- or a g^-g^+ linkage, an additional internal energy $E_{g\pm g\mp}$(CCCC) is added because these linkages bring parts of the chain near to one another, the so-called ''pentane'' effect. The rotational minima about the O–C_1 bond of the hexyloxy chains were also taken to be 0, $\pm 112°$ and a value of 124° was adopted for $\angle$COC. E'_{tg} and $E'_{g\pm g\mp}$ are used due to the presence of the oxygen in the chain. We set $E_{tg}=2400$ J/mol, $E'_{tg}=2750$ J/mol, and $E_{g\pm g\mp}=E'_{g\pm g\mp}=6500$ J/mol. These internal energies are comparable to those used for 6OCB [14] and the E_{tg} and E'_{tg} values are about a factor of 2 smaller compared with those used in 8OCB [29]. The O–C_1 bond was fixed on the ring plane for each chain to give 243 conformations. As mentioned before, the two hexyloxy chains are identical in conformation and only one chain is considered explicitly so that the Azpac molecule has a total of 243 different configurations at any time. However, it is known that the molecular fragment formed by the Pd atom and the coordinated groups (the acetylacetonate ligand and the phenyl ring *A*) is planar and rigid, and the angle (θ) formed between the ring para axes is about 7°; a dihedral angle (ϕ) of about 41° is reported between the planar fragment and the phenyl ring *B* [30]. As a result, one must consider both $\phi=+41°$ and $-41°$ in fitting the observed quadrupolar splittings. For spectral density calculations, we found that the differences for $\phi=+41°$ and $-41°$ are minimal. This is probably due to our assumption [7] of free ring rotations in modeling the ring *B* data. Hence, spectral density calculations were performed only for $\phi=41°$.

In modeling the quadrupolar splittings ($\Delta\nu_i$) of the C_i deuterons, the segmental order parameters are calculated from

$$S_{\mathrm{CD}}^{(i)}=2\Delta\nu_i/3q_{\mathrm{CD}}^{(i)}, \tag{1}$$

where $q_{\mathrm{CD}}^{(i)}$ is the quadrupolar coupling constant for the C_i deuterons and is taken as 165 and 185 kHz for methylene and ring deuterons, respectively. In the AP method, the potential energy $U(j,\Omega)$ of a molecule in a conformation *j* and a particular orientation Ω with respect to the director is given by

$$U(j,\Omega)=U_{\mathrm{int}}(j)+U_{\mathrm{ext}}(j,\Omega), \tag{2}$$

where the potential of mean torque $U_{\mathrm{ext}}(j,\Omega)$ originates from the molecular field of its neighbors, and $U_{\mathrm{int}}(j)$, the internal energy, is assumed to depend on the number (N_g)

and not the location of the *gauche* linkages in the chain, as well as $N_{g\pm g\mp}$, the number of g^+g^- and g^-g^+ linkages in the chain

$$U_{\rm int}(j)=2(N_gE_{tg}+N_{g\pm g\mp}E_{g\pm g\mp}). \tag{3}$$

The factor of 2 is to account for two hexyloxy chains in Azpac. In the principal axis (a,b,c) frame of the nuclear quadrupolar interaction and letting $S_{aa}^{n,i}$ be the segmental order parameter of the C_i–D bond (along the a axis) of the molecule with conformation n, one has

$$S_{\rm CD}^{(i)}=\sum_{n=1}^{243} p_{\rm eq}^{(n)}\left[S_{aa}^{n,i}+\frac{\eta^{(i)}}{3}(S_{bb}^{n,i}-S_{cc}^{n,i})\right], \tag{4}$$

where $\eta^{(i)}$, the asymmetry parameter of the electric field gradient, is defined by

$$\eta^{(i)}=(q_{bb}^{(i)}-q_{cc}^{(i)})/q_{aa}^{(i)}, \tag{5}$$

with $q_{aa}^{(i)}=q_{\rm CD}^{(i)}$, and $p_{\rm eq}(n)$, the equilibrium probability which specifies fraction of molecules in the conformation n, is given by

$$p_{\rm eq}(n)=\frac{1}{Z}\exp[-U_{\rm int}(n)/k_BT]Q_n, \tag{6}$$

with Q_n, the orientational partition function of conformation n, being given by

$$Q_n=\int \exp[-U_{\rm ext}(n,\Omega)/k_BT]d\Omega, \tag{7}$$

and Z, the conformation-orientational partition function, being given by

$$Z=\sum_n \exp[-U_{\rm int}(n)/k_BT]Q_n. \tag{8}$$

For the methylene deuterons, $\eta=0$ is a good approximation, while for the ring deuterons, η is taken as 0.04 [31]. Now the order parameter for a particular direction k in conformation n may be evaluated in the principal (x,y,z) frame of $U_{\rm ext}(n,\Omega)$,

$$S_{kk}^{n,i}=\sum_{\alpha}^{x,y,z} S_{\alpha\alpha}^{n}\cos^2\theta_{\alpha k}^{n,i}, \tag{9}$$

where $\theta_{\alpha k}^{n,i}$ denote angles between the $k(=a,b,c)$ axis and a principal $\alpha(=x,y,z)$ axis for the C_i–D bond, and $S_{\alpha\alpha}^{n}$, the principal order parameters of the nth rigid conformer, can easily be evaluated [32]. Of course, the constructed interaction tensor $U_{\rm ext}(n,\Omega)$ using the AP method must first be diagonalized to find the principal (x,y,z) frame for conformation n.

In calculating the ring B quadrupolar splitting, it is necessary to explicitly consider internal ring rotations, i.e., to average the splittings from the two nonequivalent deuterons in the ring due to rapid 180° ring flips. Of course, this is not done for ring A as it is part of the group coordinated to the Pd atom. The angle $\beta_{R,Q}^{B}$ between the C–D bond and ring B para axis is taken as 61°, while the $\beta_{R,Q}^{A}$ angle between the C–D bond and ring A para axis is taken to be 63°. These choices can only be rationalized by the improved fittings of static and/or dynamic observables, since the nominal value for $\angle$CD in a phenyl ring is 60°. The larger value for ring A could probably be justified by the presence of the Pd atom. Indeed we found that the fits of our relaxation data were hardly affected by making $\beta_{R,Q}^{A}=61.5°$ at the carbon 3 site. This was not the case for its corresponding quadrupolar splitting. We label the two hexyloxy chains as chain A and chain B on the ring A and ring B, respectively. To calculate ring splittings, the direction cosines in Eq. (9) must first be determined. To this end, a common molecular frame is needed to construct $U_{\rm ext}(n,\Omega)$. Although the choice of this common frame is not crucial, we find that the (x_N,y_N,z_N) frame attached to ring B is convenient (see Fig. 1). The direction cosines for the (a,b,c) axis system of each ring C–D bond in the (x_N,y_N,z_N) frame can easily be obtained and those in Eq. (9) are then obtained through a transformation from the common frame to the principal (x,y,z) frame. Besides the ring $\angle$CD angle, the direction cosines for ring A deuterons involve ϕ, and/or θ. The angle θ between the two para axes is taken to be 6° in this study.

To construct $U_{\rm ext}(j,\Omega)$, it is assumed that each conformer can be divided into a small number of rigid segments. Each segment is associated with an interaction tensor that is independent of the conformation. Suppose that the aromatic core including the C_{ar}-O bonds has an interaction tensor $\epsilon_{\alpha\beta}^{(a)}$ and each C–C (or O–C) segment has an interaction tensor $\epsilon_{\alpha\beta}^{(c)}$. By assuming both local interaction tensors to be cylindrically symmetric, only two interaction parameters X_a and X_{cc} are needed in $U_{\rm ext}(n,\Omega)$, where X_a and X_{cc} are for the core and a C–C bond, respectively. In a local (1,2,3) frame where the 3 axis is along the C_j-C_{j+1} bond, the 1 axis is in the plane bisecting the HCH angle, and the 2 axis is chosen to complete a right-handed Cartesian coordinate system, the C-D vector $\vec{V}_{\rm CD}$ is easily found. To obtain this vector in the (x_N,y_N,z_N) frame, for chain B

$$\vec{V}_{\rm CD}^{B}=R_{N,1}R_{1,2}\cdots R_{j-1,j}\vec{V}_{\rm CD}, \tag{10}$$

and for chain A

$$\vec{V}_{\rm CD}^{A}=R_{N,N'}R_{N',1}R_{1,2}\cdots R_{j-1,j}\vec{V}_{\rm CD}, \tag{11}$$

where $R_{j-1,j}$ is a rotation matrix that transforms between the jth local frame and the $(j-1)$th local frame, and $R_{N,N'}$ is a rotation matrix that transforms between the local chain A frame (x_N',y_N',z_N') to the common frame. To obtain the direction cosines in Eq. (9) for chain deuterons, Eqs. (10) and (11) need to be multiplied from the left by $R_{p,N}$ where the rotation matrix $R_{p,N}$ contains the eigenvectors $(\vec{r}_i)$ obtained in diagonalizing the total interaction tensor $\epsilon_{\alpha\beta}^{n}$ for each conformer. As the two chains are identical and noninteracting, $\epsilon_{\alpha\beta}^{n}$ is simply given by

$$\epsilon_{\alpha\beta}^{n}=\epsilon_{\alpha\beta}^{(a)}+R_{N,N'}R_{N',1}\lambda_{2\beta}^{n}R_{N',1}^{-1}R_{N,N'}^{-1}+R_{N,1}\lambda_{2\beta}^{n}R_{N,1}^{-1}, \tag{12}$$

where the first term is for the molecular core, the second and third terms are for chain *A* and chain *B*, respectively, and

$$\lambda^n_{\alpha\beta}=\sum_{j=2}^{7} R_{1,2}\cdots R_{j-1,j}\epsilon^{(c)}_{\alpha\beta}R^{-1}_{j-1,j}\cdots R^{-1}_{1,2}. \qquad (13)$$

A similar approach in constructing $\epsilon^n_{\alpha\beta}$ has been used before [15]. Finally, we use Eqs. (6)–(11) to compute $S^{(i)}_{\mathrm{CD}}$ in Eq. (4) separately for $\phi=\pm 41°$, and the calculated $S^{(i)\mathrm{calc}}_{\mathrm{CD}}$ is given by

$$S^{(i)\mathrm{calc}}_{\mathrm{CD}}=\frac{1}{2}[S^{(i)}_{\mathrm{CD}}(\phi=41°)+S^{(i)}_{\mathrm{CD}}(\phi=-41°)]. \qquad (14)$$

By fitting the measured segmental order parameters $S^{(i)}_{\mathrm{CD}}$ to Eq. (14) at each temperature, the interaction parameters X_a and X_{cc} can be determined. Furthermore, the order parameters $\langle P_2\rangle$ and $\langle S_{xx}-S_{yy}\rangle$ for an ''average'' conformer of the molecule can be evaluated [9]. In solving the rotational diffusion problem of a ''rigid'' molecule, Nordio *et al.* [8] used a second rank potential of mean torque $U(\beta)$,

$$\frac{U(\beta)}{k_BT}=a_{20}\left(\frac{3}{2}\cos^2\beta-\frac{1}{2}\right), \qquad (15)$$

where β is the angle between the molecular long axis and the director. The above potential is specified by the second rank coefficient a_{20}, which can be determined from a knowledge of the nematic order parameter $\langle P_2\rangle$.

The spectral density $J_m(m\omega)$ may be evaluated by Fourier transforming the autocorrelation function $G_m(t)$,

$$J^{(i)}_m(m\omega)=\frac{3\pi^2}{2}(q^{(i)}_{\mathrm{CD}})^2\int_0^\infty G_m(t)\cos(m\omega t)dt, \qquad (16)$$

where $G_m(t)$ may be expressed in terms of the Wigner rotation matrix $D^2_{mn}(\Omega)$ in the fluctuating spin Hamiltonian

$$G_m(t)=\langle D^2_{m0}[\Omega_{LQ}(0)]D^{2*}_{m0}[\Omega_{LQ}(t)]\rangle, \qquad (17)$$

where the angle brackets denote an ensemble average and the Euler angles $\Omega_{LQ}(t)$ specify the orientation of the principal axes of the electric-field-gradient (EFG) tensor (the η parameter is set to zero here) with respect to the laboratory frame whose z_L axis is defined by the external magnetic field. To evaluate $G_m(t)$, one needs to transform the EFG tensor through successive coordinates [9] to allow for possible internal rotations and overall reorientations. For ring *A* of Azpac, there is no internal motion, and its deuterons would only sense the rotational diffusion of the molecule as a whole (i.e., diffusive motions of the long molecular z_d axis, see Fig. 1). From our previous study, the z_d axis was found [6] to lie between the two para axes and make an angle of 1° with the para axis of the more ordered ring *A*. We assume the same axis system to diagonalize the rotational diffusion tensor with principal elements $D_\parallel$ and $D_\perp$, which are the rotation diffusion constants about the z_d axis and of the z_d axis, respectively. According to the Nordio model, the spectral densities for deuterons at sites 3 and 5 in ring *A* are given by (using the notation of Ref. [22])

$$J^{(i)}_m(m\omega)=\frac{3\pi^2}{2}(q^{(R)}_{\mathrm{CD}})^2\sum_n [d^2_{n0}(\beta^{(i)}_{d,Q})]^2 \times\sum_k \frac{(\Psi^2_{mnn})_K(\Phi^2_{mnn})_K}{(\Phi^2_{mnn})^2_K+m^2\omega^2}, \qquad (18)$$

where *m* and *n* represent the projection indices of a rank 2 tensor in the laboratory (z_L) and molecular (z_d) frames, respectively; $\Phi^2_{mnn}/D_\perp$, the decay constants, are the eigenvalues of the rotation diffusion operator (Γ) matrix and $(\Psi^2_{mnn})_K$, the relative weights of the decaying exponentials, are the corresponding eigenvectors; $i=3A$ or $5A$ for the deuteron at carbon 3 or carbon 5 site. Now $\beta^{(3A)}_{d,Q}=\beta^A_{R,Q}-1°$ and $\beta^{(5A)}_{d,Q}=\beta^A_{R,Q}+1°$. Note that the Γ operator contains explicitly the orienting potential and the rotational diffusion constants $D_\parallel$ and $D_\perp$. For the deuterons on ring *B*, the above equation must be modified to include internal ring rotations with a diffusion constant D_R. The resulting spectral densities for ring rotations in a small-step diffusive limit are given by

$$J^{(B)}_m(m\omega)=\frac{3\pi^2}{2}(q^{(R)}_{\mathrm{CD}})^2\sum_n\sum_{m_R}[d^2_{m_R0}(\beta^B_{R,Q})]^2[d^2_{nm_R}(\theta')]^2 \times\sum_K \frac{(\Psi^2_{mnn})_K[(\Phi^2_{mnn})_K+m^2_RD_R]}{[(\Phi^2_{mnn})_K+m^2_RD_R]^2+m^2\omega^2}, \qquad (19)$$

where $\theta'=\theta-1°$. Finally, to treat correlated internal rotations in chains *A* and *B*, one should realize that both chains behave the same way in their respective local (x'_N,y'_N,z'_N) and (x_N,y_N,z_N) frames under our assumption of identical chains. A further coordinate transformation to the (x_d,y_d,z_d) frame makes the final spectral densities for the deuterons on chain *A* and chain *B* different. Thus, the relaxation behaviors of the two hexyloxy chains are slightly different simply due to a geometric factor. According to our decoupled model, the spectral densities for the methylene deuterons in chain *B* are given by [10]

$$J^{(p)}_m(m\omega)=\frac{3\pi^2}{2}(q^{(p)}_{\mathrm{CD}})^2\sum_n\sum_{j=1}^{243}\left|\sum_{l=1}^{243} d^2_{m_N0}(\beta^{(p)l}_{N,Q})d^2_{nm_N}(\theta') \times\exp[-im_N\alpha^{(p)l}_{N,Q}]x^{(1)}_l x^{(j)}_l\right| \times\sum_K^2 \frac{(\Psi^2_{mnn})_K[(\Phi^2_{mnn})_K+|\lambda_j|]}{[(\Phi^2_{mnn})_K+|\lambda_j|]^2+m^2\omega^2}, \qquad (20)$$

where $\beta^{(p)l}_{N,Q}$ and $\alpha^{(p)l}_{N,Q}$ are the polar angles of the C_p–D bond of the conformer *l* in a local (x_N,y_N,z_N) frame and θ' is the angle between the z_N and z_d axes (i.e., 185°). λ_j and $\vec{x}^{(j)}$ are the eigenvalues and eigenvectors obtained by diagonalizing the symmetrized transition rate matrix of the master rate equation. A similar equation to Eq. (20) can be written for chain *A* by changing (x_N,y_N,z_N) to (x'_N,y'_N,z'_N) and m_N to m'_N. θ' now represents the angle between the z'_N axis and the z_d axis (i.e., $\theta'=1°$). Equations (18)–(20) are used to model the derived spectral densities from Azpac-d_4 and Azpac-d_{26}. At each temperature, there are six motional model parameters. These are $D_\parallel$, $D_\perp$, D_R and the three jump rate constants k_1, k_2, and k_3.

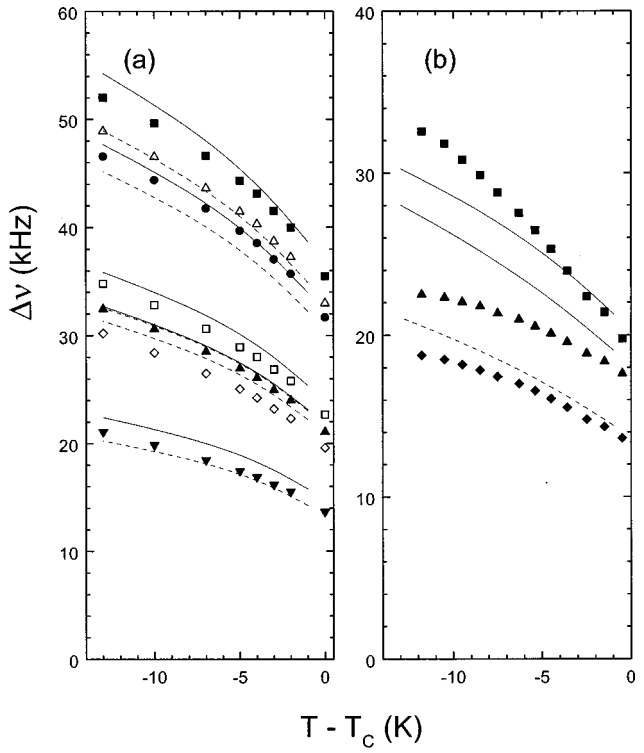

FIG. 2. Plots of quadrupolar splittings versus the temperature. Solid and dashed curves represent fits for chain (or ring) *A* and chain (or ring) *B*, respectively. (a) Azpac-d_{26}: closed squares, circles, up triangles, and down triangles denote $C_1^{A,B}$, C_2^B, $C_3^A(C_4^B)$, and $C_5^{A,B}$, respectively. Open up triangles, squares, and diamonds denote C_2^A, C_4^A, and C_3^B, respectively. The calculated curves (drawn through theoretical points) starting from the top are for C_1^A, C_1^B, C_2^A, C_2^B, C_3^A, C_4^A, C_3^B, C_4^B, C_5^A, and C_5^B, respectively. Note that the experimental splittings of C_3 and C_4 are reversed from those predicted by the theory. (b) Azpac-d_4: squares, triangles, and diamonds denote C_5^A, C_3^A, and $C_{3,5}^B$, respectively. The calculated curves starting from the top are for C_5^A, C_3^A, and $C_{3,5}^B$, respectively.

III. RESULTS AND DISCUSSION

The experimental details have been reported before [6,7]. Unfortunately, the NMR relaxation data collected in Azpac-d_{26} did not cover the same wide temperature range as Azpac-d_4. Since we want to interpret both the splittings and spectral densities from these samples, we are limited to a narrow temperature range of about 7° near $T_C(=368\ \mathrm{K})$ when considering the relaxation data of Azpac. Figure 2 shows the quadrupolar splittings as a function of temperature in the nematic phase of Azpac-d_4 and Azpac-d_{26}. Mean field calculations of segmental order parameter profile at each temperature according to Eq. (14) were carried out to model the observed quadrupolar splittings in Fig. 2. An optimization routine (AMOEBA) was used [33] to minimize the sum squared error *f*,

$$f=\sum_i \left(|S_{\mathrm{CD}}^{(i)}|-|S_{\mathrm{CD}}^{(i)\mathrm{Calc}}|\right)^2, \tag{21}$$

where the sum over *i* includes all the methylene deuterons in C_1 to C_5 from both chains, as well as ring *A* and *B* deuterons. The *f* values at different temperatures are of the order of 3×10^{-3}. The fits to the quadrupolar splittings are shown in Fig. 2 as solid and dashed curves for chain (ring) *A* and chain (ring) *B*, respectively. It should be noted that the previous assignment of $\Delta\nu_4>\Delta\nu_3$ [7] is not predicted by the theory here. The incorrect prediction of splittings at C_3 and C_4 has occurred in previous mean field calculations for other liquid crystals [14,28]. In addition, the peculiar temperature behavior of ring *A* splittings is not reproduced. This could perhaps be explained by a slight temperature effect on the distortion of the ring *A* structure. In the temperature range where we study the relaxation behaviors, the fits are quite good, as evidenced in Fig. 3 for T-$T_C=5$ K. The derived $\langle P_2\rangle$ values are comparable to those obtained previously based on the Azpac-d_4 data only [6], and the derived interaction parameters X_a and X_{cc} are sufficiently accurate for evaluating the equilibrium probability $P_{\mathrm{eq}}(n)$ needed to describe chain dynamics below. We plot $\langle P_2\rangle$ and $\langle S_{xx}-S_{yy}\rangle$ for an ''average'' conformer of the Azpac molecule, as well as X_a and X_{cc} versus the temperature in Fig. 4. The molecular biaxial order parameter $\langle S_{xx}-S_{yy}\rangle$ is found to be quite small, making Nordio model a good approximation for describing molecular reorientations.

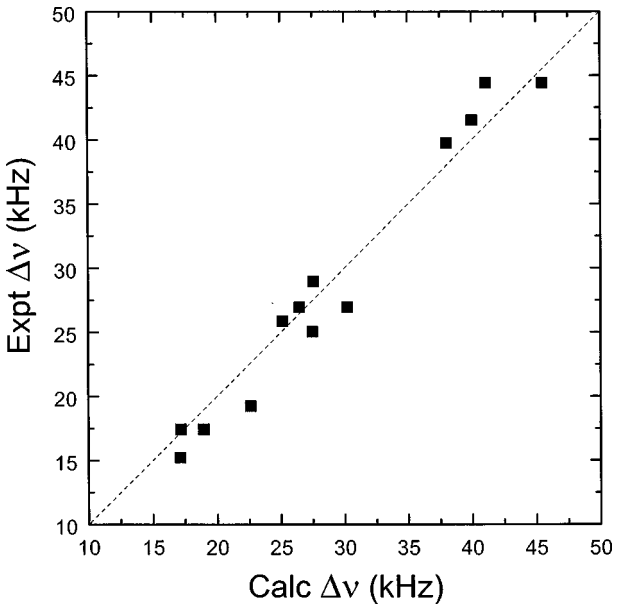

FIG. 3. Plot of experimental quadrupolar splittings vs calculated quadrupolar splittings of Azpac-d_4 and Azpac-d_{26} at 363 K.

Figure 5 reproduces the spectral densities of Azpac versus the difference in temperature from T_C. Some sinusoidal variations in the spectral density data are not real and they simply reflect relatively large experimental uncertainties. Indeed smoothed data are used as experimental values for model fittings. To model spectral densities from the core and chain deuterons (excluding the methyls), AMOEBA was used to minimize the mean-squared percent deviation (F) in an individual target analysis (i.e., analyzing one temperature at a time),

$$F=\sum_k \sum_m \left[\frac{J_m^{(k)\mathrm{calc}}(m\omega)-J_m^{(k)\exp t}(m\omega)}{J_m^{(k)\exp t}(m\omega)}100\right]^2, \tag{22}$$

where the sum over *k* includes all methylene and ring data

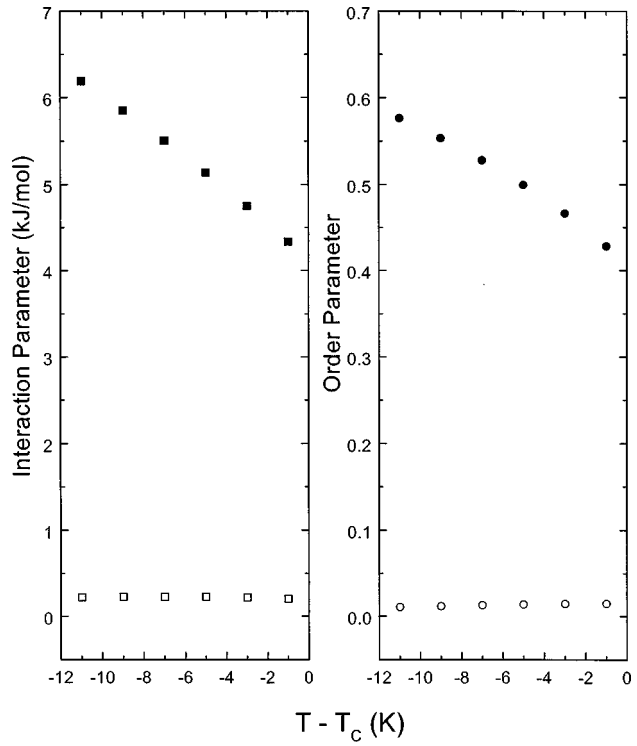

FIG. 4. Plots of interaction parameters X_a (closed squares) and X_{cc} (open squares), as well as order parameters for an average conformer $\langle P_2 \rangle$ (closed circles) and $\langle S_{xx} - S_{yy} \rangle$ (open circle) vs the temperature.

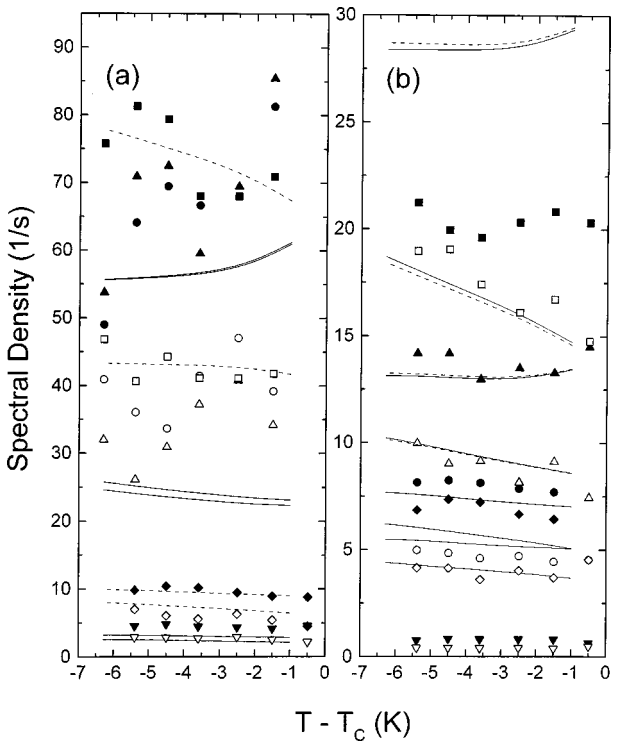

FIG. 5. Plots of spectral density data at 46 MHz for Azpac. Closed and open symbols represent $J_1(\omega)$ and $J_2(2\omega)$, respectively. (a) Squares, up triangles, and circles denote ring data at $C^B_{3,5}$, C^A_3, and C^A_5, respectively. Diamond and down triangle denote chain data at C^B_3 and $C^{A,B}_5$, respectively. (b) Squares, up triangles, circles, diamonds, and down triangles denote chain data at $C^{A,B}_1$, $C^{A,B}_2$, $C^A_3(C^B_4)$, C^A_4, and $C^{A,B}_6$, respectively. Solid curves denote calculated $J_1(\omega)$ and $J_2(2\omega)$ in chain (ring) *A*, while dashed curves denote calculated $J_1(\omega)$ and $J_2(2\omega)$ in chain (ring) *B*. The predicted curves in (a) (drawn through theoretical points) from the top are ring $J_1(\omega)$ of $C^B_{3,5}$, C^A_5, and C^A_3, ring $J_2(2\omega)$ of $C^B_{3,5}$, C^A_5, and C^A_3, chain $J_1(\omega)$ and $J_2(2\omega)$ of C^B_3 and chain $J_1(\omega)$ and $J_2(2\omega)$ of $C^{A,B}_5$, while in (b) from the top down are for $J_1(\omega)$ of C^B_1 and C^A_1, $J_2(2\omega)$ of C^A_1 and C^B_1, $J_1(\omega)$ of C^B_2 and C^A_2, $J_2(2\omega)$ of C^A_2 and C^B_2, $J_1(\omega)$ of $C^A_3(C^B_4)$, $J_2(2\omega)$ of $C^A_3(C^B_4)$, $J_1(\omega)$ of C^A_4, and $J_2(2\omega)$ of C^A_4.

and $m=1$ or 2. The fitting quality factor Q in the spectral density calculations is given by the percent mean-squared deviation

$$Q = \frac{\sum_k \sum_m [J_m^{(k)\mathrm{calc}}(m\omega) - J_m^{(k)\exp t}(m\omega)]^2}{\sum_k \sum_m [J_m^{(k)\exp t}(m\omega)]^2} \times 100. \tag{23}$$

Since the ^{2}H-NMR signals from carbon 3 of chain *A* and carbon 4 of chain *B* are completely overlapped, making separate determination of their individual T_1's impossible and the calculated spectral densities for these two sites are quite different, averages of the calculated J_1's and J_2's from these two sites are used to compare with the observed spectral density values. At each temperature, there are 26 spectral densities (with some of them being identical due to spectral limitations) to derive the six motional parameters. We found that the Q values are better at the low temperature end than those near T_C, varying from 1.4% to 6%. The poor Q values are mainly due to rather scattered ring *A* data obtained near T_C (e.g., at 365 K, $Q=4\%$). Indeed when better spectral density data are available and in particular over a wider temperature range, a global target analysis [34] could be carried out. The fits to the spectral density data are shown in Fig. 5 as solid [for chain (ring) *A*] and dashed [for chain (ring) *B*] curves. As seen in this figure, the predicted differences in the spectral densities at the corresponding sites of chain *A* and chain *B* as well as for carbons 3 and 5 in ring *A* are in general quite small, and may be impossible to discern experimentally. Figure 6 shows the site dependences of $J_1(\omega)$ and $J_2(2\omega)$ at 361.7 K and their calculated values using the decoupled model. On the whole, the available spectral density data from Azpac-d_4 and Azpac-d_{26} are reasonably fitted with our simplified motional model for a nematogen having two side chains of same lengths. Thus it would appear justifiable to use the major assumption of identical configurations for the two noninteracting side chains in Azpac. Figure 7 summarizes the rotational diffusion constants and jump constants at several temperatures examined in the present study. Because of the narrow temperature range, it is impossible to get a handle on their temperature dependences. For example, $D_\parallel$ is essentially independent of temperature and the D_R values for ring *B* are around 1×10^9 s^{-1} as found in other liquid crystals [9]. As expected, $D_\parallel > D_\perp$. It is, however, interesting to see that both $D_\parallel (\simeq 2\times10^7$ s$^{-1})$ and $D_\perp (3-5\times10^6$ s$^{-1})$ are at least an order of magnitude smaller than in conventional rodlike liquid crystals [9]. We note that $D_\parallel$ and $D_\perp$ could only be estimated previously [7] based solely on

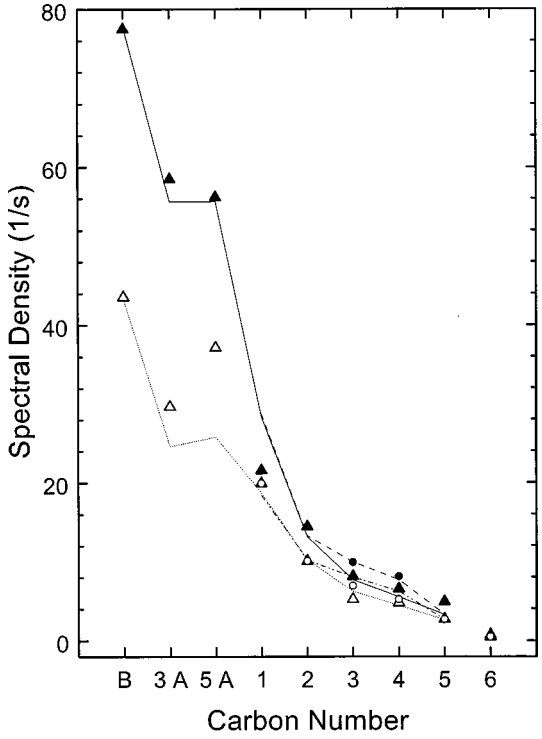

FIG. 6. Variation of the spectral densities $J_1(\omega)$ (closed symbols) and $J_2(2\omega)$ (open symbols) with the deuteron position in the nematic phase of Azpac ($T=361.7$ K). Triangles and circles denote data from chains (rings) *A* and *B*, respectively. Solid and dotted lines are predictions for chain (ring) *A*, while dashed and dot-dashed lines for chain (ring) *B*. Note that the chain data at this temperature were obtained by extrapolating the experimental data.

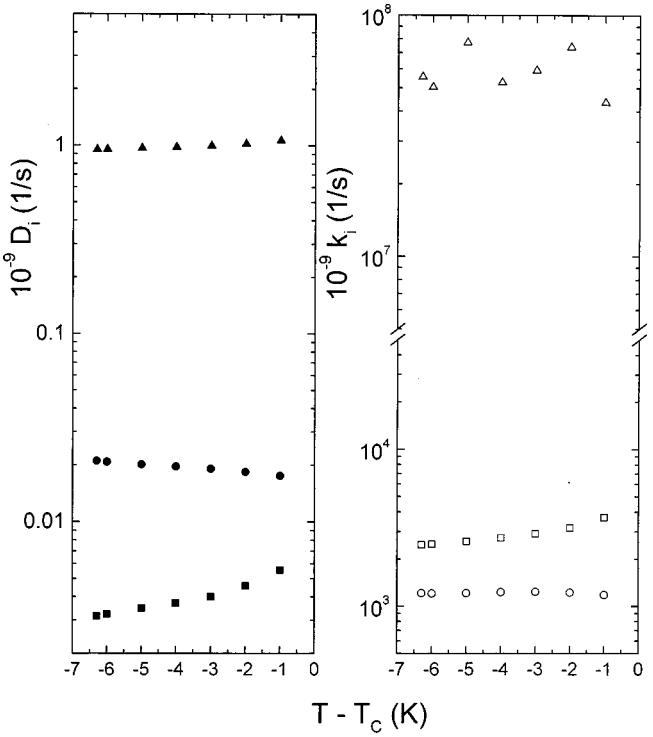

FIG. 7. Plots of rotational diffusion constants $D_\perp$ (closed squares), $D_\parallel$ (closed circles), and D_R (closed triangles), as well as jump constants k_1 (open squares), k_2 (open circles), and k_3 (open triangles) vs the temperature in the nematic phase of Azpac.

the ring data of Azpac-d_4. As demonstrated here, the inclusion of both the ring and chain data in an individual target analysis can remedy this difficulty. The jump constants k_1, k_2, and k_3 behave similar to other liquid crystals studied so far. Again the three-bond motion ($k_3 \simeq 6\times10^{16}$ s^{-1}) is the fastest internal motion. To illustrate the error limits in each of the model parameter, we use the data at 361.7 K. The error limit for a particular model parameter was estimated by varying the one under consideration while keeping all other parameters identical to those for the minimum F value to give an approximate doubling in the F value. We found that any lower $D_\perp$ value ($D_\perp = 3.15\times10^6$ s^{-1}) did not affect the fits and its upper error limit was 7.75×10^6 s^{-1}. The error limits for $D_\parallel$ ranged between 1.3×10^7 s^{-1} to 3.0×10^7 s^{-1}. In estimating the error limits for k_3, no upper limit could be found as the fits were insensitive to values higher than 5.6×10^{16} s^{-1}. Its lower error limit was 5.2×10^{13} s^{-1}. The error limits for k_1 were 1.5×10^{12} s^{-1} and 6.1×10^{12} s^{-1}, while those for k_2 were 7×10^{11} s^{-1} and 3×10^{12} s^{-1}. Finally correlations among various model parameters are addressed [35]. The correlation coefficient between $D_\parallel$ and $D_\perp$ is 0.93 and between one of these with D_R is very small. The correlation between one of jump constants and either $D_\parallel$ or $D_\perp$ is between 0.2 and 0.3, while between one of these jump constants and D_R is zero. Correlations between pairs of jump constants are in the range of 0.80–0.85.

IV. SUMMARY

A quantitative analysis of both the quadrupolar splittings and spectral density data from two isotopomers of the metallomesogen Azpac is reported in this work. The proposed motional model is used to account for a rodlike liquid crystal molecule having two identical chains like Azpac. Indeed to reduce the number of possible configurations in Azpac both in the AP method and decoupled model for conformational dynamics, the two side chains are assumed to take the same configuration for the purpose of fitting the quadrupolar splittings, and only one chain (either the *A* or *B* chain) is considered explicitly for explaining the deuteron spin relaxation in Azpac-d_{26}. As a result, Azpac has 243 conformations and the transition rate matrix has the dimensions 243×243 and can be handled in a reasonable computing time. It is fortunate and surprising how well the assumption works for Azpac. Relaxation data at a different frequency when available may serve as a further check. The derived motional parameters, though over a small temperature range, are physically plausible and represent new physical properties obtained in a metallomesogen. We hope that this paper would stimulate further NMR work, in particular relaxation measurements, in this class of metal containing liquid crystals.

ACKNOWLEDGMENTS

The financial support of the Natural Science and Engineering Research Council of Canada is gratefully acknowledged. We (R.Y.D. and C.A.V.) thank NATO for a collaborative research grant (No. CRG970537) for a project on metallomesogen.

[1] S. A. Hudson and P. M. Maitlis, Chem. Rev. **93**, 861 (1993); B. Donnio and D. W. Bruce, Struct. Bonding (Berlin) **95**, 193 (1999).
[2] C. Versace, G. Cipparrone, D. Lucchetta, D. Pucci, and M. Ghedini, Mol. Cryst. Liq. Cryst. Sci. Technol., Sect. A **212**, 313 (1992).
[3] C. Versace, V. Formoso, D. Lucchetta, D. Pucci, C. Ferrero, M. Ghedini, and R. Bartolino, J. Chem. Phys. **98**, 8507 (1993).
[4] N. Scaramuzza, M. C. Pagnotta, and D. Pucci, Mol. Cryst. Liq. Cryst. Sci. Technol., Sect. A **239**, 195 (1994).
[5] A. G. Petrov, A. T. Ionescu, C. Versace, and N. Scaramuzza, Liq. Cryst. **19**, 169 (1995).
[6] L. Calucci, D. Catalano, M. Ghedini, N. L. Jones, D. Pucci, and C. A. Veracini, Mol. Cryst. Liq. Cryst. Sci. Technol., Sect. A **290**, 87 (1996).
[7] L. Calucci, C. Forte, M. Geppi, and C. A. Veracini, Z. Naturforsch., A: Phys. Sci. **53**, 427 (1998).
[8] P. L. Nordio and P. Busolin, J. Chem. Phys. **55**, 5485 (1971); P. L. Nordio, G. Rigatti, and U. Segre, *ibid.* **56**, 2117 (1972).
[9] R. Y. Dong, *Nuclear Magnetic Resonance of Liquid Crystals* (Springer-Verlag, New York, 1997).
[10] L. Calucci, M. Geppi, C. A. Veracini, and R. Y. Dong, Chem. Phys. Lett. **296**, 357 (1998).
[11] R. Y. Dong and G. M. Richards, J. Chem. Soc., Faraday Trans. **88**, 1885 (1992).
[12] G. Q. Cheng and R. Y. Dong, J. Chem. Phys. **89**, 3308 (1988).
[13] R. Y. Dong and X. Shen, J. Phys. Chem. **101**, 4673 (1997).
[14] X. Shen and R. Y. Dong, J. Chem. Phys. **108**, 9177 (1998).
[15] X. Shen, R. Y. Dong, N. Boden, R. J. Bushby, P. S. Martin, and A. Wood, J. Chem. Phys. **108**, 4324 (1998).
[16] R. Y. Dong, Phys. Rev. A **43**, 4310 (1991); R. Y. Dong and G. M. Richards, Chem. Phys. Lett. **171**, 389 (1990).
[17] A. Ferrarini, G. J. Moro, and P. L. Nordio, Liq. Cryst. **8**, 593 (1990).
[18] J. W. Emsley, G. R. Luckhurst, and C. P. Stockley, Proc. R. Soc. London, Ser. A **381**, 117 (1982).
[19] J. H. Freed, J. Chem. Phys. **41**, 2077 (1964); W. Huntress, Jr., Adv. Magn. Reson. **4**, 1 (1970).
[20] J. M. Bernassau, E. P. Black, and D. M. Grant, J. Chem. Phys. **76**, 253 (1982).
[21] J. Bulthuis and L. Plomp, J. Phys. (Paris) **51**, 258 (1990).
[22] R. Tarroni and C. Zannoni, J. Chem. Phys. **95**, 4550 (1991).
[23] E. Berggren, R. Tarroni, and C. Zannoni, J. Chem. Phys. **99**, 6180 (1993); E. Berggren and C. Zannoni, Mol. Phys. **85**, 299 (1995).
[24] R. R. Vold and R. L. Vold, J. Chem. Phys. **88**, 1443 (1988).
[25] R. Y. Dong, Mol. Phys. **141**, 349 (1986); D. E. Woessner, J. Chem. Phys. **36**, 1 (1962).
[26] P. A. Beckmann, J. W. Emsley, G. R. Luckhurst, and D. L. Turner, Mol. Phys. **54**, 97 (1986).
[27] P. J. Flory, *Statistical Mechanics of Chain Molecules* (Wiley, New York, 1969).
[28] C. J. R. Counsell, J. W. Emsley, N. J. Heaton, and G. R. Luckhurst, Mol. Phys. **54**, 847 (1985).
[29] R. Y. Dong, Phys. Rev. E **60**, 5631 (1999).
[30] M. C. Etter and A. R. Siedle, Am. Cryst. Assoc. Ser. 2 **8**, 29 (1980); J. Am. Chem. Soc. **105**, 641 (1983).
[31] R. Ambrosetti, D. Catalano, C. Forte, and C. A. Veracini, Z. Naturforsch. Teil A **41**, 431 (1986).
[32] G. R. Luckhurst, C. Zannoni, P. L. Nordio, and U. Segre, Mol. Phys. **30**, 1345 (1975).
[33] W. H. Press, B. P. Flannery, S. A. Teukolsky, and W. T. Vetterling, *Numerical Recipes* (Cambridge University Press, Cambridge, England, 1986).
[34] R. Y. Dong, Mol. Phys. **88**, 979 (1996).
[35] W. C. Hamilton, *Statistics in Physical Science* (The Ronald Press, New York, 1964).